Electronic Supplementary Material (ESI) for Physical Chemistry Chemical Physics.

Efficient Sampling of Molecular Orientations for Cu(II)-based DEER on protein labels

Zikri Hasanbasri,[a] Nicholas A. Moriglioni [a] and Sunil Saxena [a]

Department of Chemistry, University of Pittsburgh, Pittsburgh, PA, 15260, USA

* To whom correspondence should be addressed: ORCID: 0000-0001-9098-6114, Phone (412) 624-8680. Email: sksaxena@pitt.edu

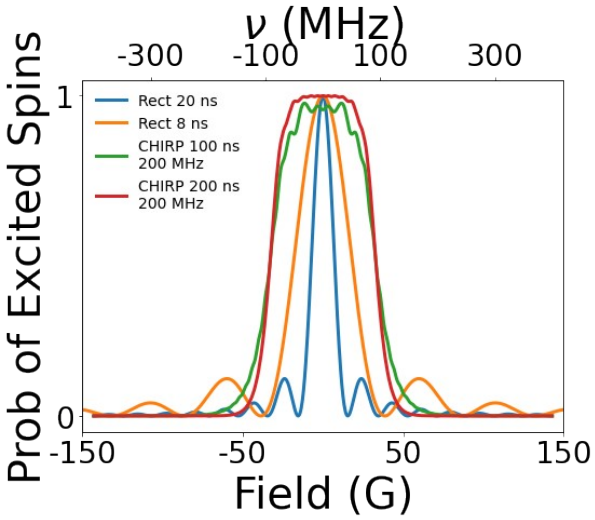

Figure S1. Functions for the probability of spin excitation as a function of either field or frequency relative to the pulse frequency. The probability functions were calculated from the inversion profiles of 20 ns Rectangular (blue), 8 ns Rectangular (orange), 100 ns 200 MHz CHIRP (green), and 200 ns 200 MHz CHIRP (red).

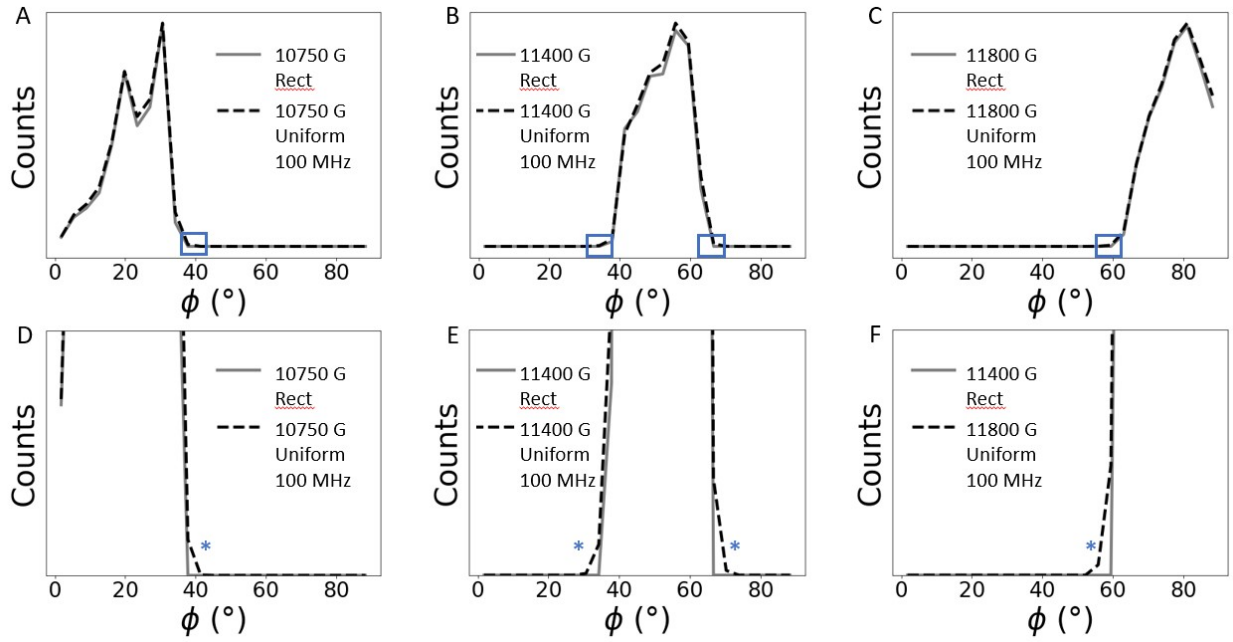

Figure S2. 20 ns rectangular pulse and a uniform excitation 100MHz pulse were set at three different fields (10750 G, 11400 G, 11800 G) across the dHis-Cu(II) spectrum, as referred to in Figure 3 of the main text. At each field, the sampled ϕ angles were calculated and plotted for the rectangular and uniform excitation pulse, represented as the dashed black line and the solid gray line, respectively. The distributions of sampled ϕ angles were normalized to the maximum count, as shown in panels A-C. Panels D-F show zoomed-in versions of the ϕ distributions. The blue rectangle and the blue star mark the region where the ϕ angles were sampled by the minor lobes of the rectangular pulse.

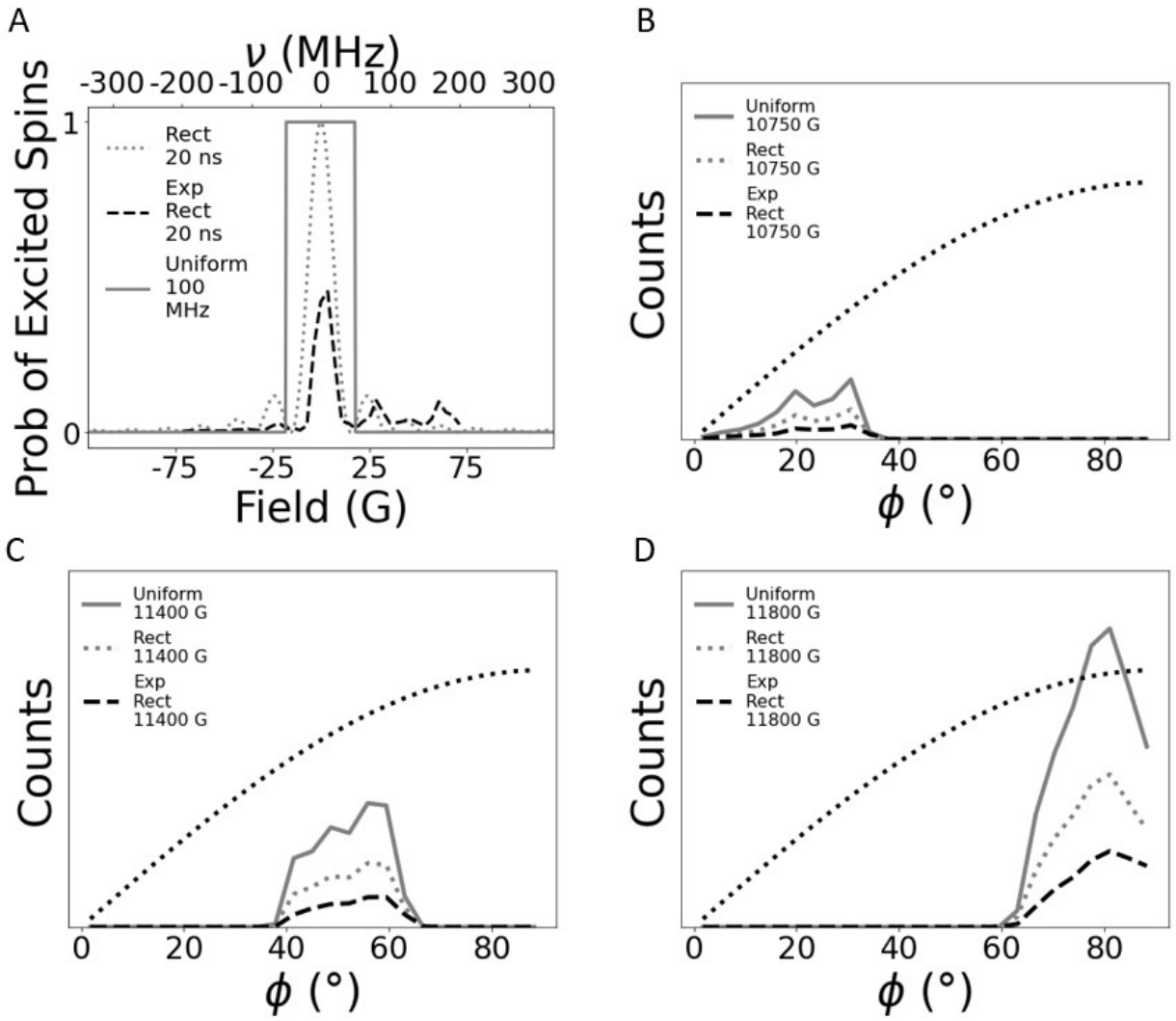

Figure S3. A) Functions for the probability of spin excitation as a function of either field or frequency relative to the pulse frequency. The probability functions were calculated from the inversion profiles of uniform excitation 100 MHz (solid gray), 20 ns Rectangular (dotted gray), and the experimental 20 ns Rectangular (dashed black). The experimental inversion profile was obtained using the previous protocol[1]. The pulse was set at -400 MHz away from the central resonator frequency of the Bridge12 QLP resonator. The three pulses were applied at three fields; 10750 G (B), 11400 G (C), and 11800 G (D). At each field, the sampled ϕ angles were calculated and plotted for the three pulses. Overall, the three pulses sampled similar ranges of ϕ angles. Furthermore, the resonator distortion does not change the range of sampled ϕ angles.

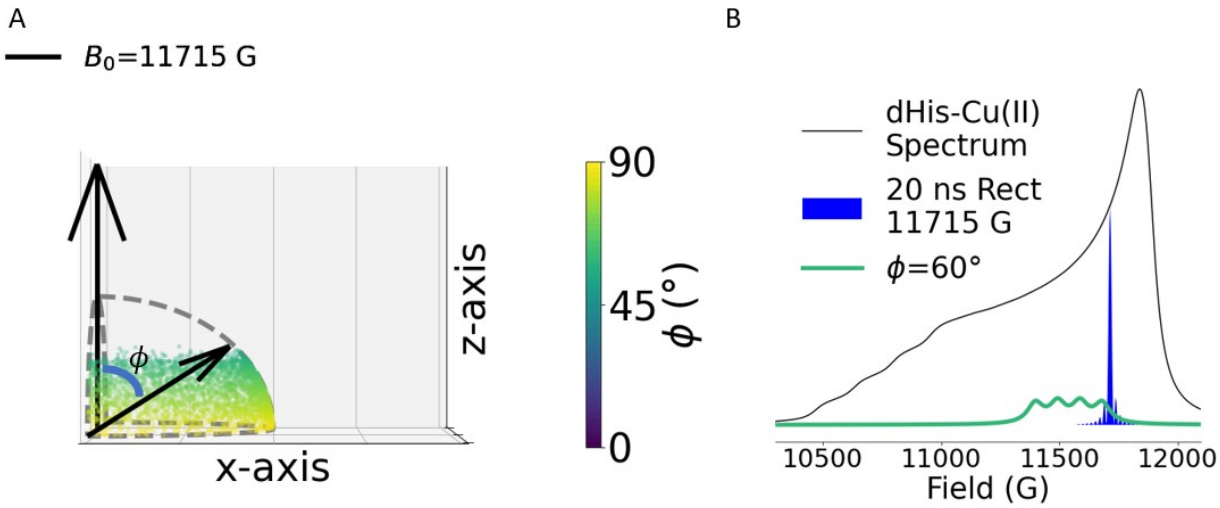

Figure S4. A scatter plot of the spins excited by a 20 ns Rectangular pulse at 11715 G. The cartesian coordinates of each dot represent the ϕ angle of the spin. The color of each dot corresponds to the ϕ angle of the spin. B) Representation of the excitation of the sample by a 20 ns Rectangular pulse (shaded blue area) at 11715 G. For reference, the simulated dHis-Cu(II) spectrum is shown as the black line. The green line represents the spectral lineshape of a spin with a ϕ angle of 60°. Overall, at 11715 G, the 20 ns Rectangular pulse can sample ϕ angles from ~60° to 90°.

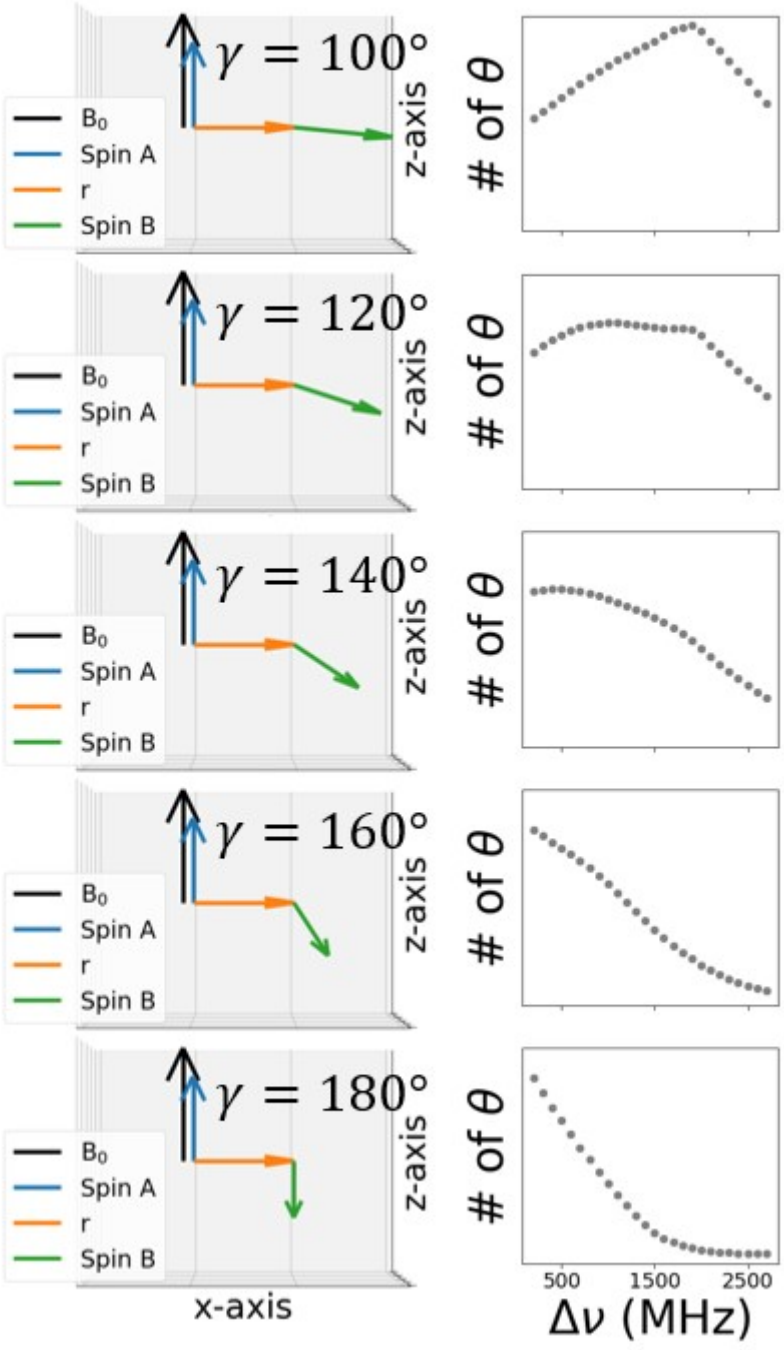

Figure S5. Analysis of five different cases where the angle between the $g_{\parallel}$-axes of the two spins was incremented by 20° in the range of 90° to 180°, defined by the parameter γ. The organization of r and the two $g_{\parallel}$-axes of the spins are depicted on the left panels as orange, blue, and green, respectively. DEER simulations were done on each case with a variety of $\Delta\nu$ values. The number of excited θ as a function of $\Delta\nu$ is plotted as gray dots on the right panels. The optimal $\Delta\nu$ varies in each case. As the orientations of the two spins deviate, the optimal $\Delta\nu$ increases to excite the two spins with differing resonant fields properly.

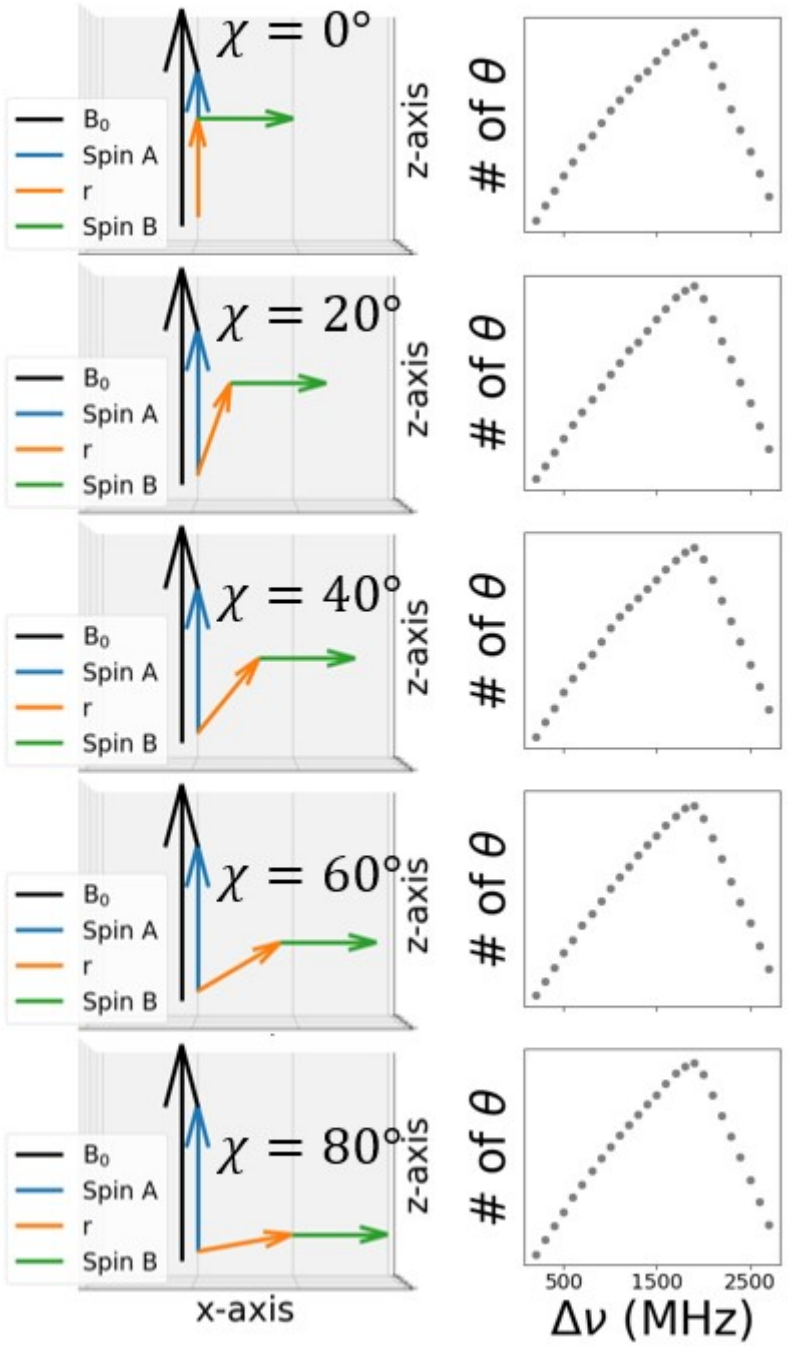

Figure S6. Analysis of five different cases where the angle between the $g_{\parallel}$-axis Spin A and r was incremented by 20°, defined by the parameter γ. The organization of r and the two $g_{\parallel}$-axes of the spins are depicted on the left panels as orange, blue, and green, respectively. In all of these cases, γ and η were set as 90° and 0°, respectively. DEER simulations were done on each case with a variety of $\Delta\nu$ values. The number of excited θ as a function of $\Delta\nu$ is plotted as gray dots on the right panels. The optimal $\Delta\nu$ remains consistent at 1900 MHz across all five cases. More importantly, the optimal $\Delta\nu$ and the $\Delta\nu$ curve are

identical to results from Figure 5E where γ is 80°. Overall, χ minimally affects the efficiency of exciting spin-pairs.

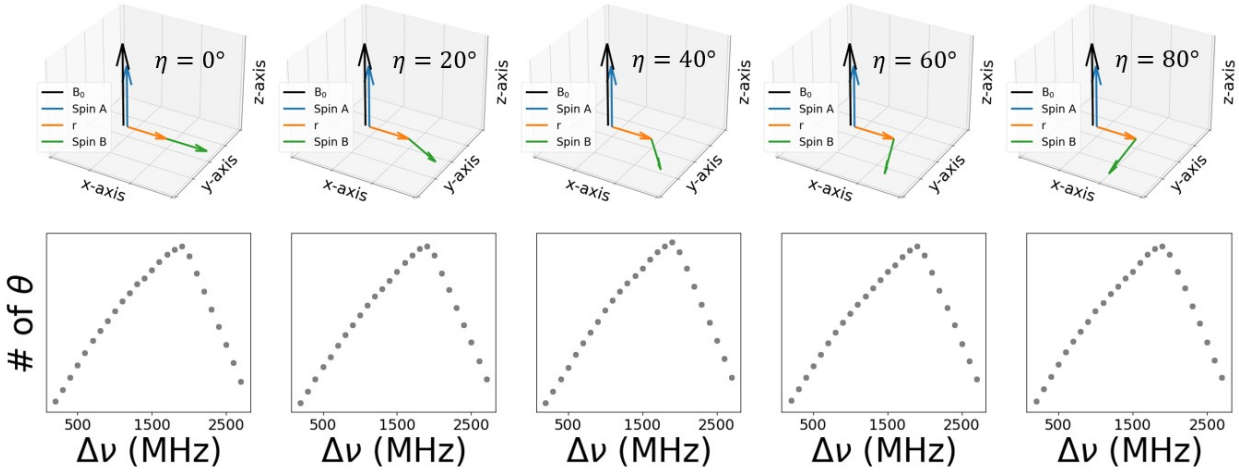

Figure S7. Analysis of five different cases where the angle between the $g_{\perp}$-axes of the two spins was incremented by 20°, defined by the parameter η. The organization of r and the two $g_{\parallel}$-axes of the spins are depicted on the top panels as orange, blue, and green, respectively. In these cases, both χ and γ were set as 90°. DEER simulations were done on each case with a variety of $\Delta\nu$ values. The number of excited θ as a function of $\Delta\nu$ is plotted as gray dots on the right panels. The optimal $\Delta\nu$ remains consistent at 1900 MHz across all five cases. More importantly, the optimal $\Delta\nu$ and the $\Delta\nu$ curve are identical to results from Figure 5E where γ is 80°. Overall, γ minimally affects the efficiency of exciting spin-pairs.

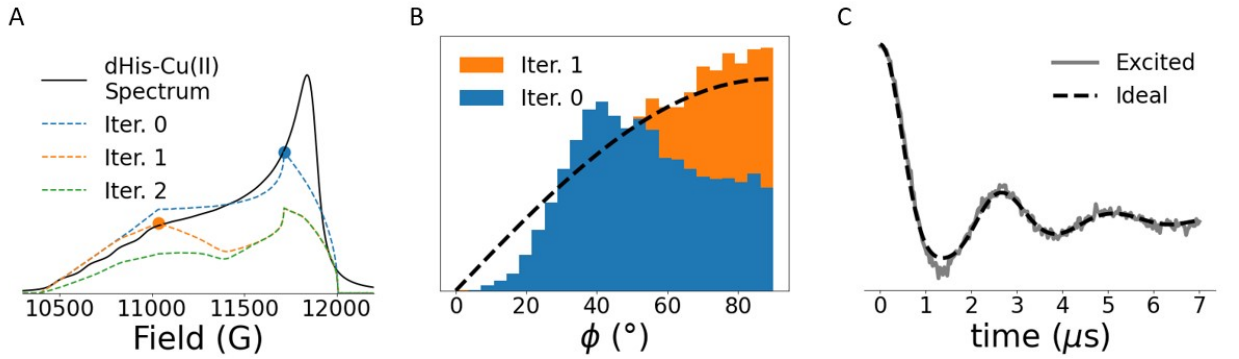

Figure S8. A) Φ-curve analysis, where the DEER simulations used Φ-curve 900 MHz. Each iteration is a Φ-curve obtained from spin pairs that were not yet excited by DEER simulations from previous iterations. The maximum of each Φ-curve, marked by colored dots, was identified as the most promising field for simulating DEER at a given iteration. B) The distribution of sampled θ from the simulated DEER performed at the fields shown in panel A after each iteration. C) The simulated DEER signal after performing the DEER experiments at the fields identified in panel A.

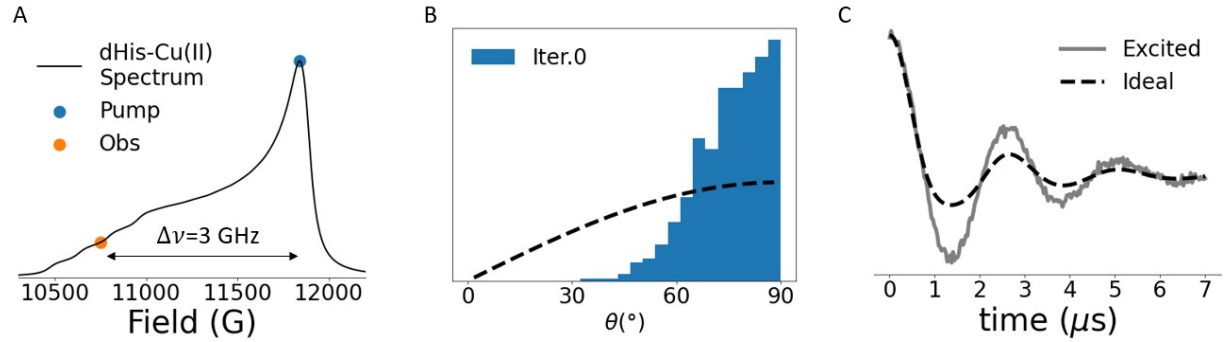

Figure S9. A) A DEER was simulated by setting the pump pulse at the $g_{\perp}$ of the dHis-Cu(II) spectrum (blue dote) and the observer pulse at the $g_{\parallel}$ of the spectrum (orange dot). The two pulses are separated by 3 GHz. B) The distribution of sampled θ from the simulated DEER performed at the fields shown in panel A after each iteration. C) The simulated DEER signal after performing the DEER experiments at the fields identified in panel A.

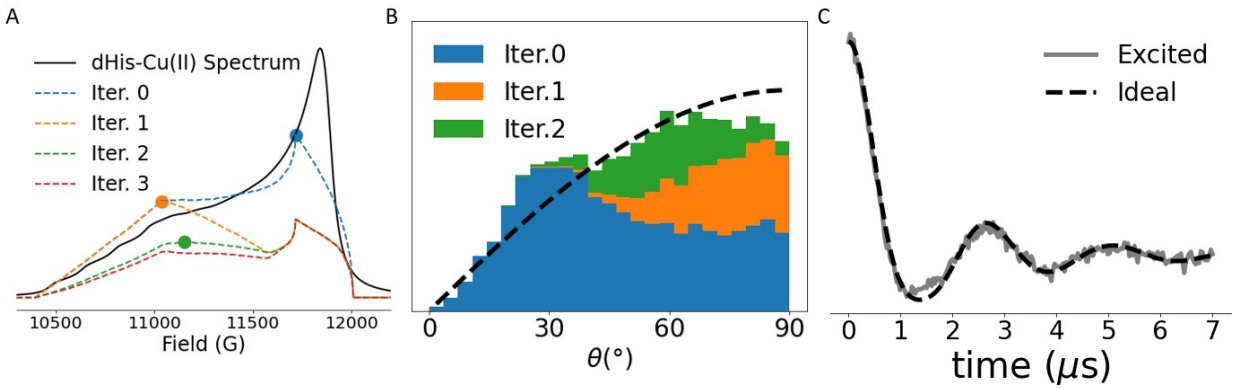

Figure S10. A) Φ-curve analysis, where the DEER simulations used Φ-curve 200 MHz. Each iteration is a Φ-curve obtained from spin pairs that were not yet excited by DEER simulations from previous iterations. The maximum of each Φ-curve, marked by colored dots, was identified as the most promising field for simulating DEER at a given iteration. B) The distribution of sampled θ from the simulated DEER performed at the fields shown in panel A after each iteration. C) The simulated DEER signal after performing the DEER experiments at the fields identified in panel A.

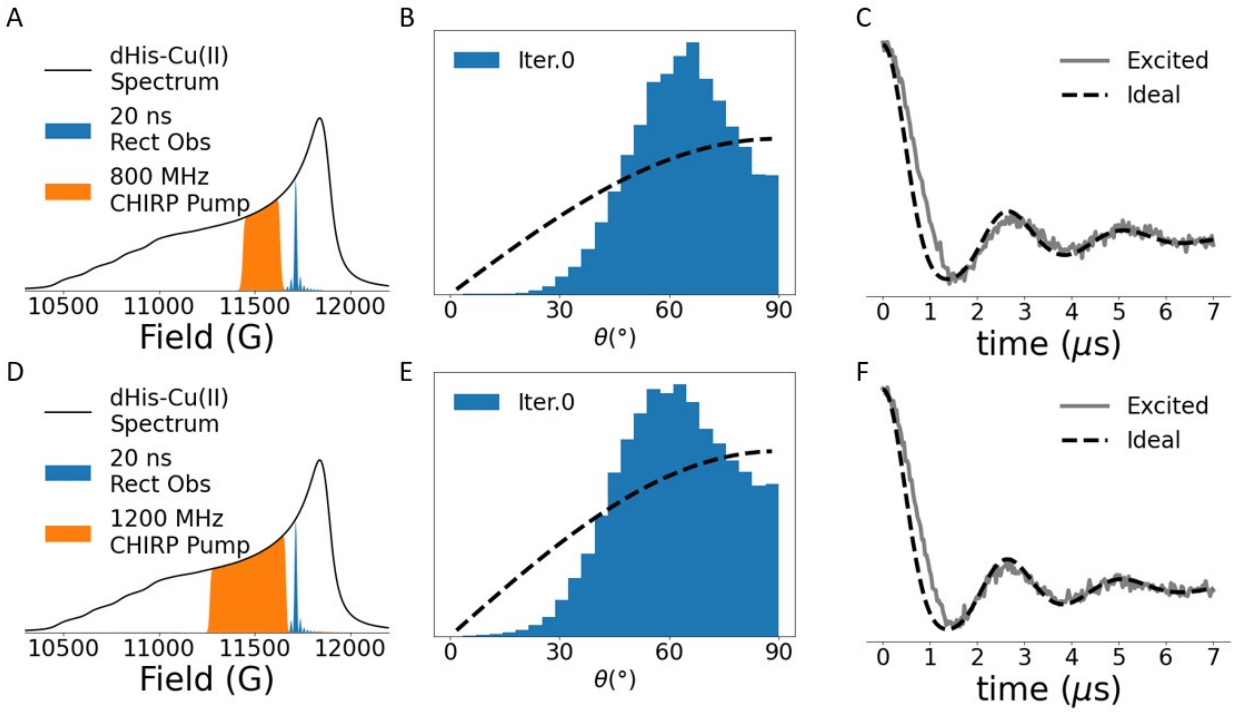

Figure S11. DEER was simulated by setting the pump pulse as either 800 MHz CHIRP (A) or 1200 MHz CHIRP (D). The distribution of sampled θ from the two simulated DEER performed are shown as blue histograms in panels B and E. Panels C and F show the simulated DEER signal.

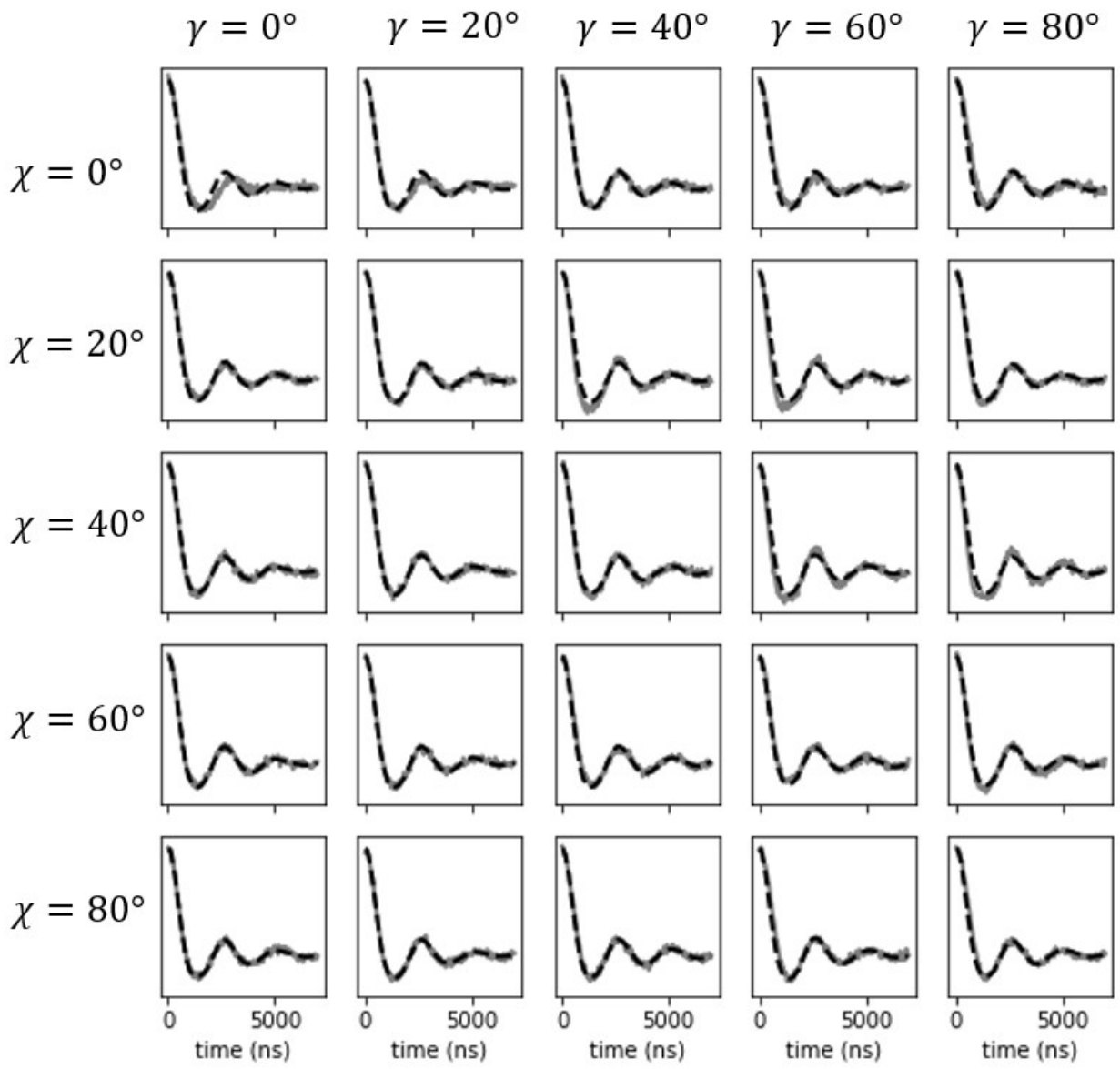

Figure S12. The simulated and ideal DEER time traces were obtained for different angles of χ and γ while η is 20°. The simulated DEER was obtained using the two identified fields in Figure 6A in the main text, given a 300 MHz frequency offset between observer and pump frequencies.

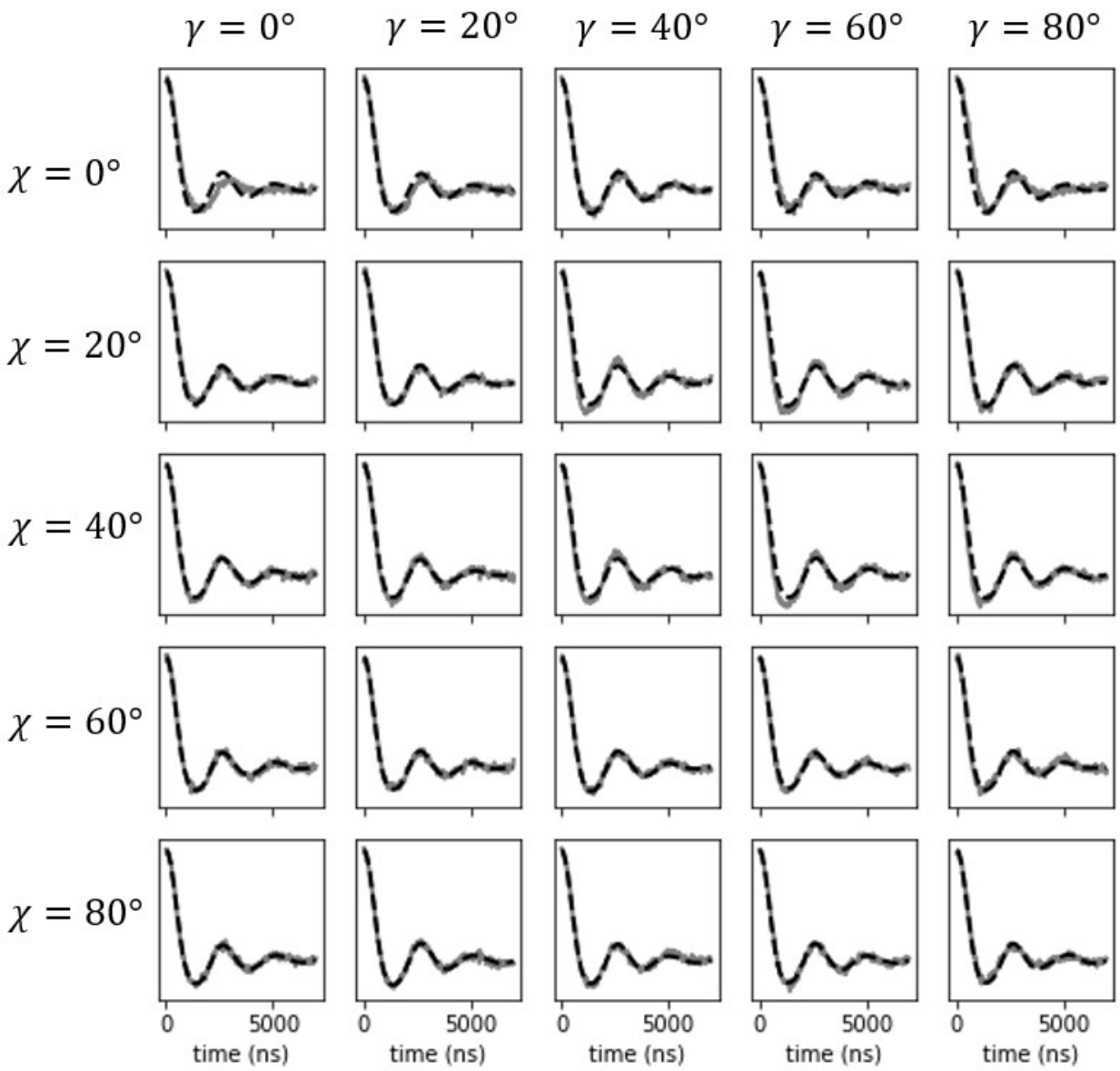

Figure S13 The simulated and ideal DEER time traces were obtained for different angles of χ and γ while η is 40°. The simulated DEER was obtained using the two identified fields in Figure 6A in the main text, given a 300 MHz frequency offset between observer and pump frequencies.

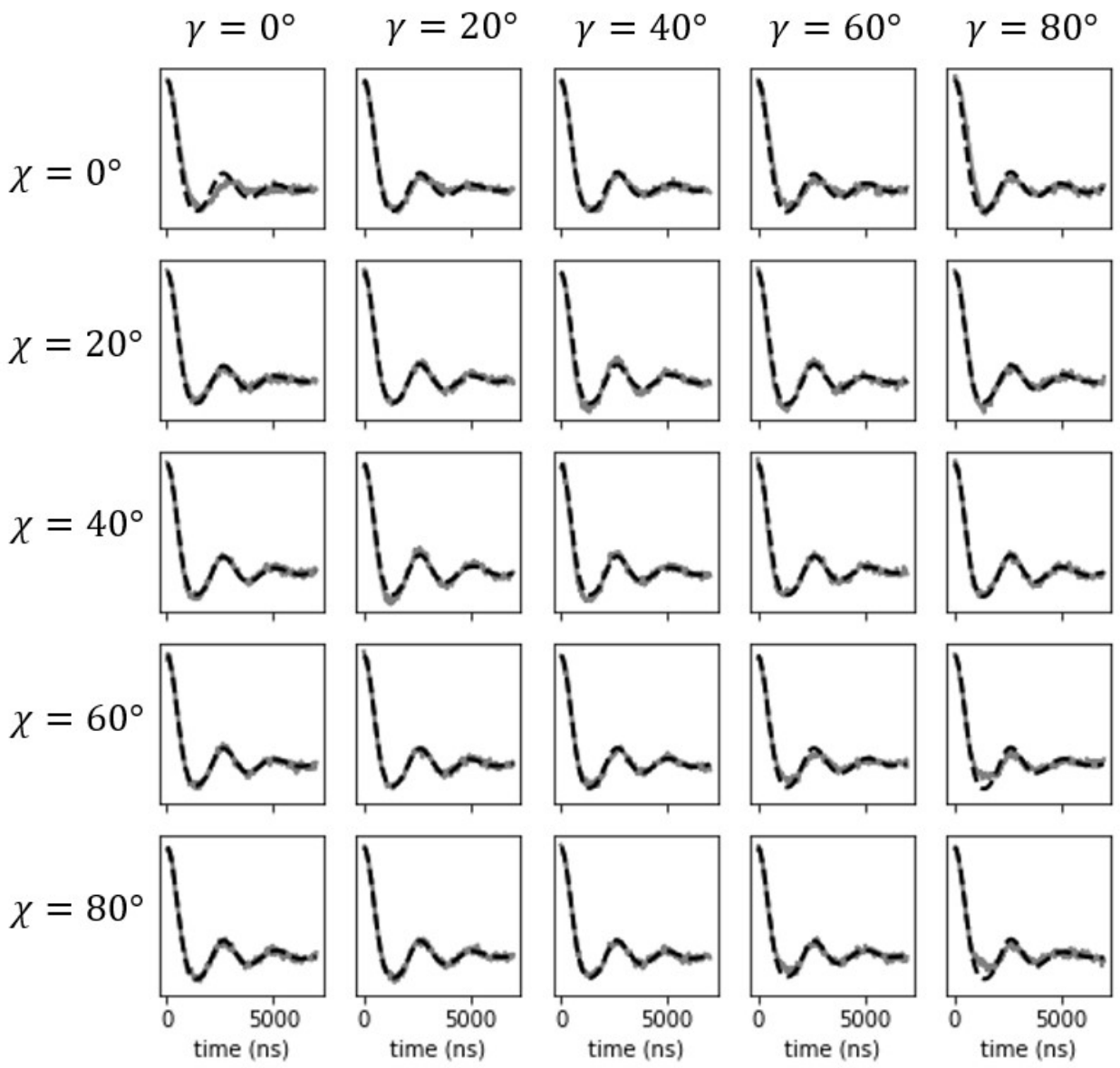

Figure S14. The simulated and ideal DEER time traces were obtained for different angles of χ and γ while η is 60°. The simulated DEER was obtained using the two identified fields in Figure 6A in the main text, given a 300 MHz frequency offset between observer and pump frequencies.

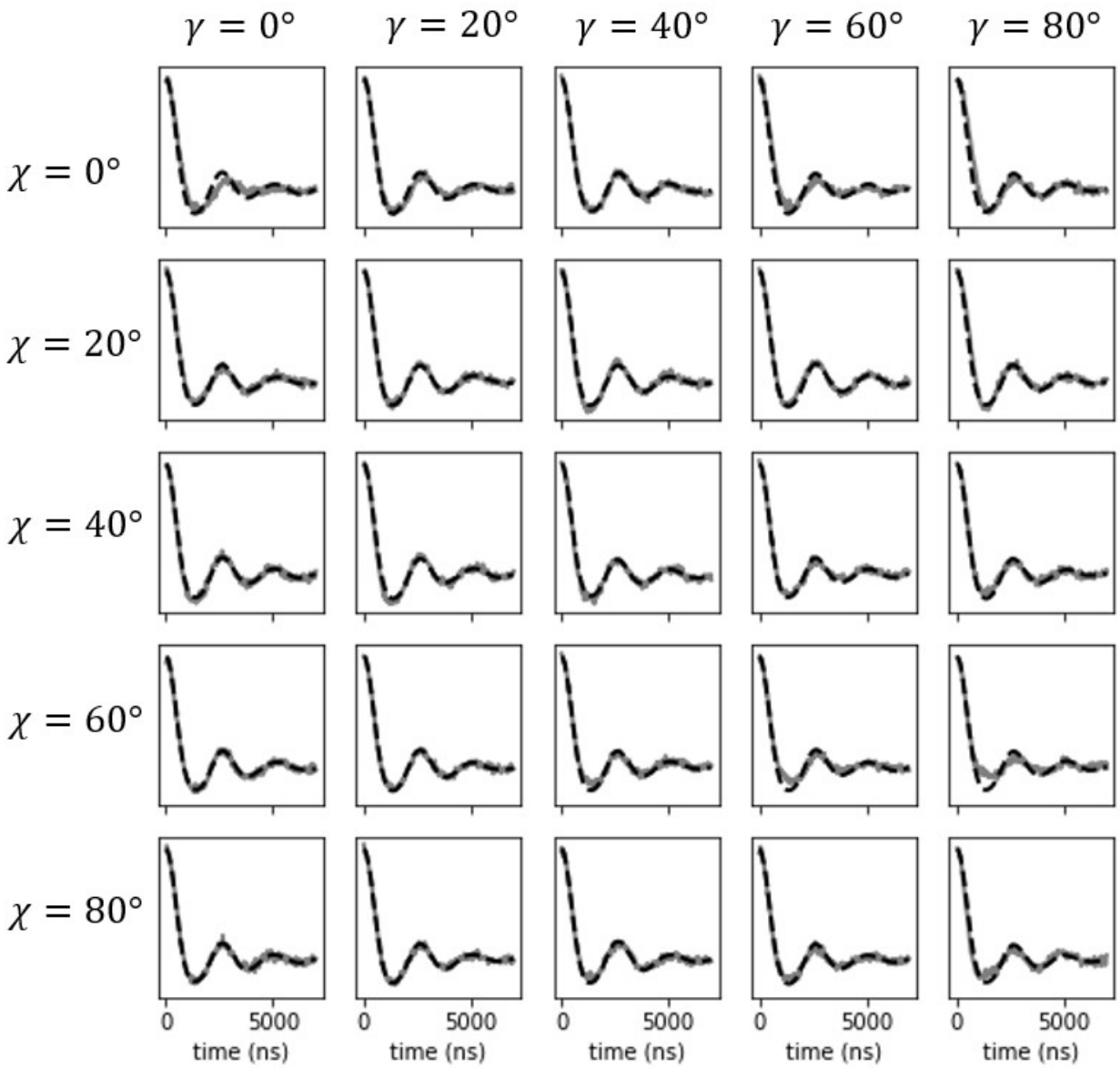

Figure S15. The simulated and ideal DEER time traces were obtained for different angles of χ and γ while η is 80°. The simulated DEER was obtained using the two identified fields in Figure 6A in the main text, given a 300 MHz frequency offset between observer and pump frequencies.

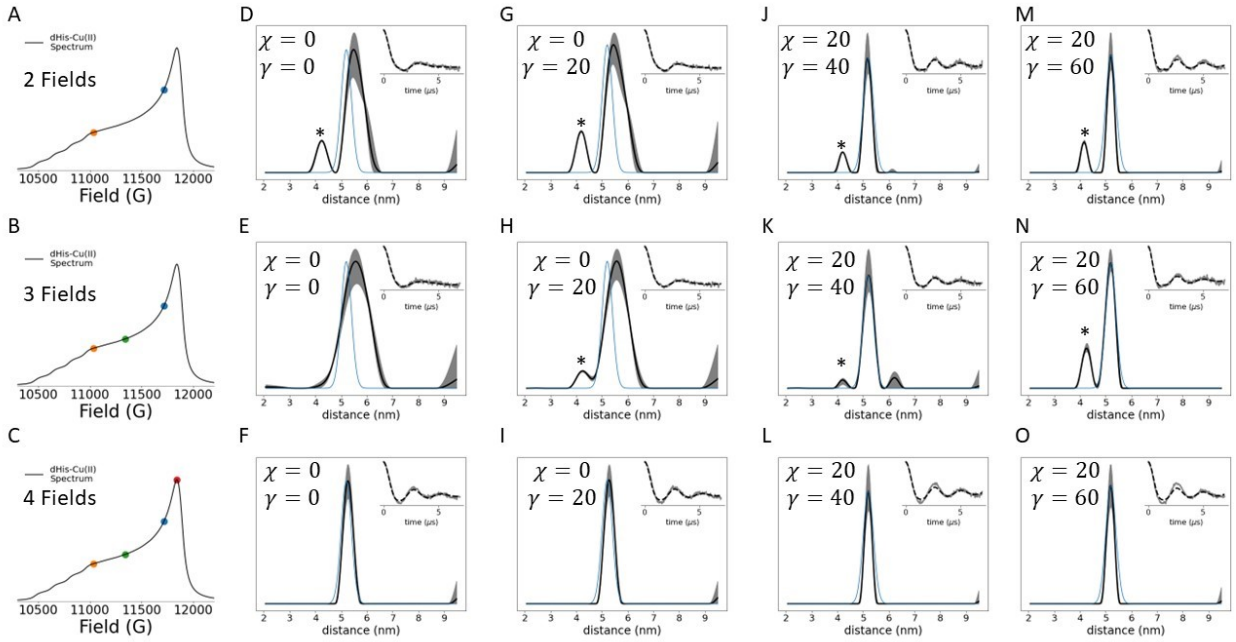

Figure S16. DEER simulations were performed at 2 (A), 3 (B), or 4 (C) field positions, marked by the colored dots. The blue, orange, green, and red dots represent 124 G, 803 G, 500 G, and 0 G lower than the maximum of the dHis-Cu(II) spectrum. The simulations were done on four cases; χ=0°, γ=0° (D-F); χ=0°, γ=20° (G-I); χ=20°, γ=40° (J-L); and χ=20°, γ=60° (M-O). All four cases have η of 0°. These parameters refer to relative orientations that show residual orientational selectivity effects after simulating DEER at two fields, as depicted in Figure 7 in the main text. The insets in panels D-O show the fitting of the simulated DEER signal using the Tikhonov Regularization algorithm in DeerAnalysis[2]. The gray line represents the simulated DEER signal, while the dashed black line represents the fitting. The extracted distance distributions are shown in the main panels as the solid black line, while the gray line represents the error in the distribution. Minor distributions that manifest from residual orientational selectivity effects are marked with *. For comparison, the ideal distance distributions in the simulations are shown as the blue line.

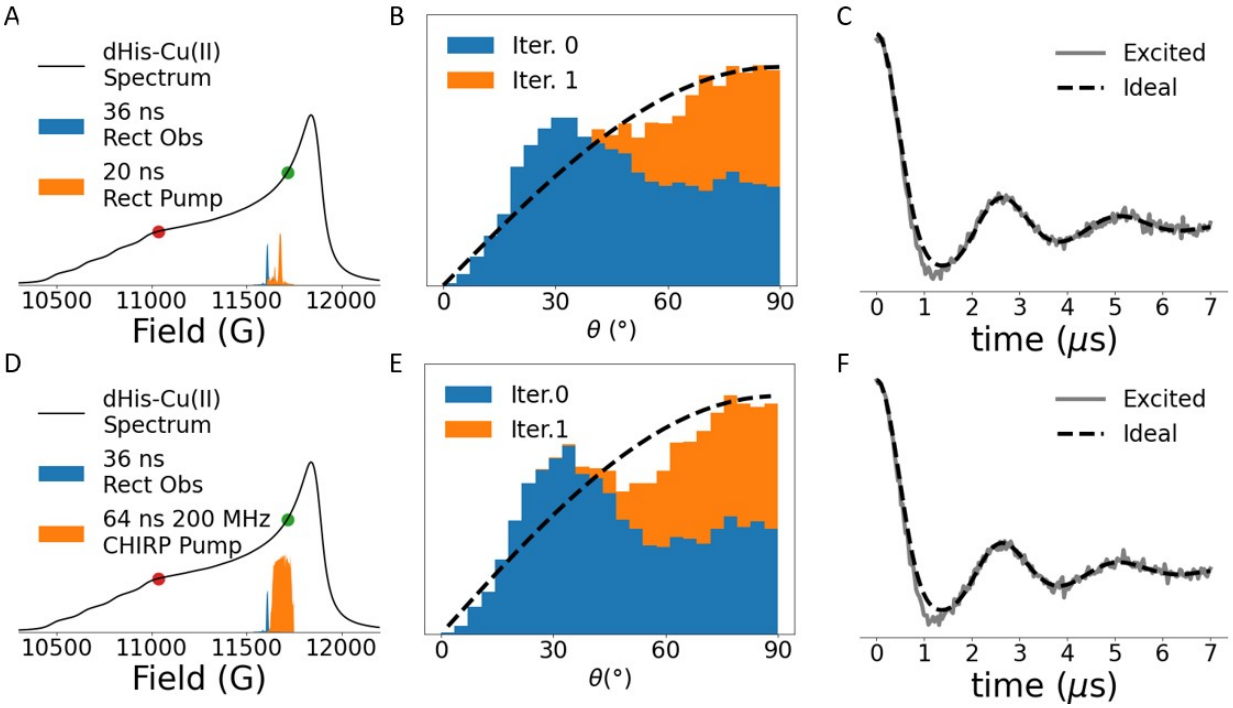

Figure S17. DEER was simulated by setting the pump pulse as either 20 ns Rectangular (A) or 64 ns 200 MHz CHIRP (D). In both cases, the observer pulse was set as 36 ns Rectangular. The simulations were done at 124 G and 803 G lower than the dHis-Cu(II) spectrum maximum. The inversion profiles were obtained experimentally using the previous protocol[1]. The parameters used in the simulations were meant to replicate the experimental setup described in Figure 8 of the main text. The distribution of sampled θ from the two simulated DEER performed are shown as blue histograms in panels B and E. Panels C and F show the simulated DEER signal. Overall, these simulations further support the feasibility of obtaining orientation-averaged DEER.

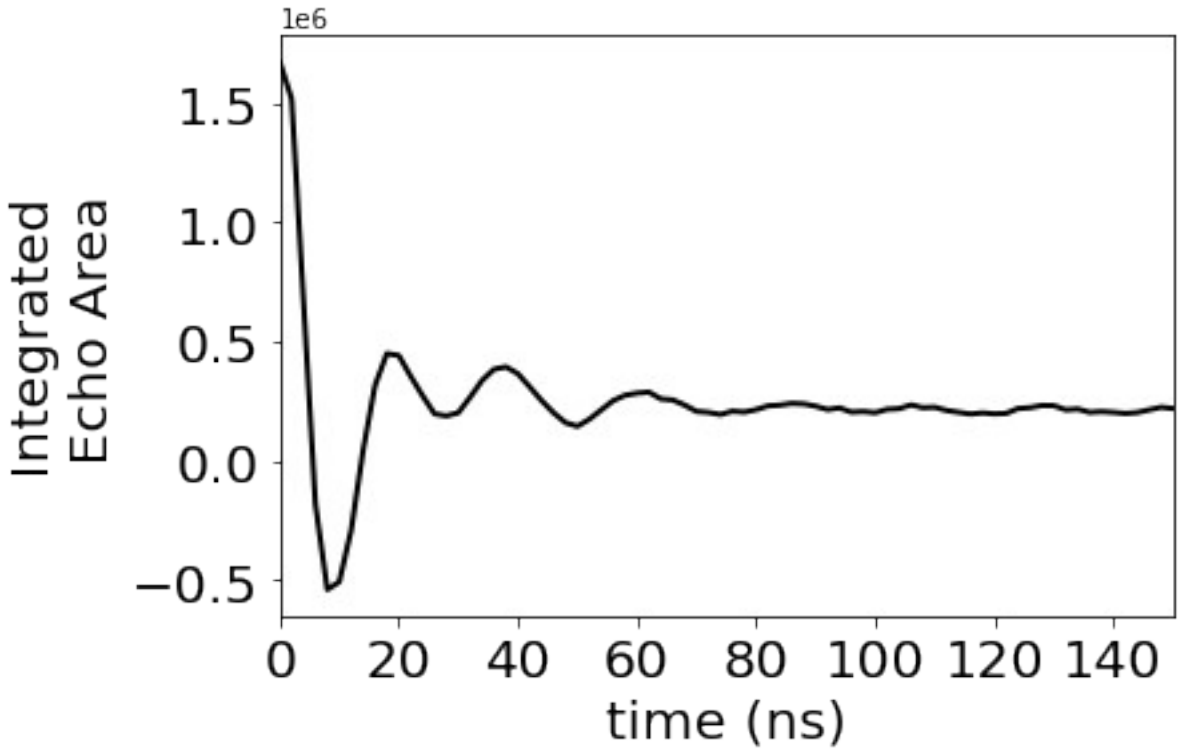

Figure S18. Nutation experiment at the central ν of the B12 resonator with attenuation of 8 dB.

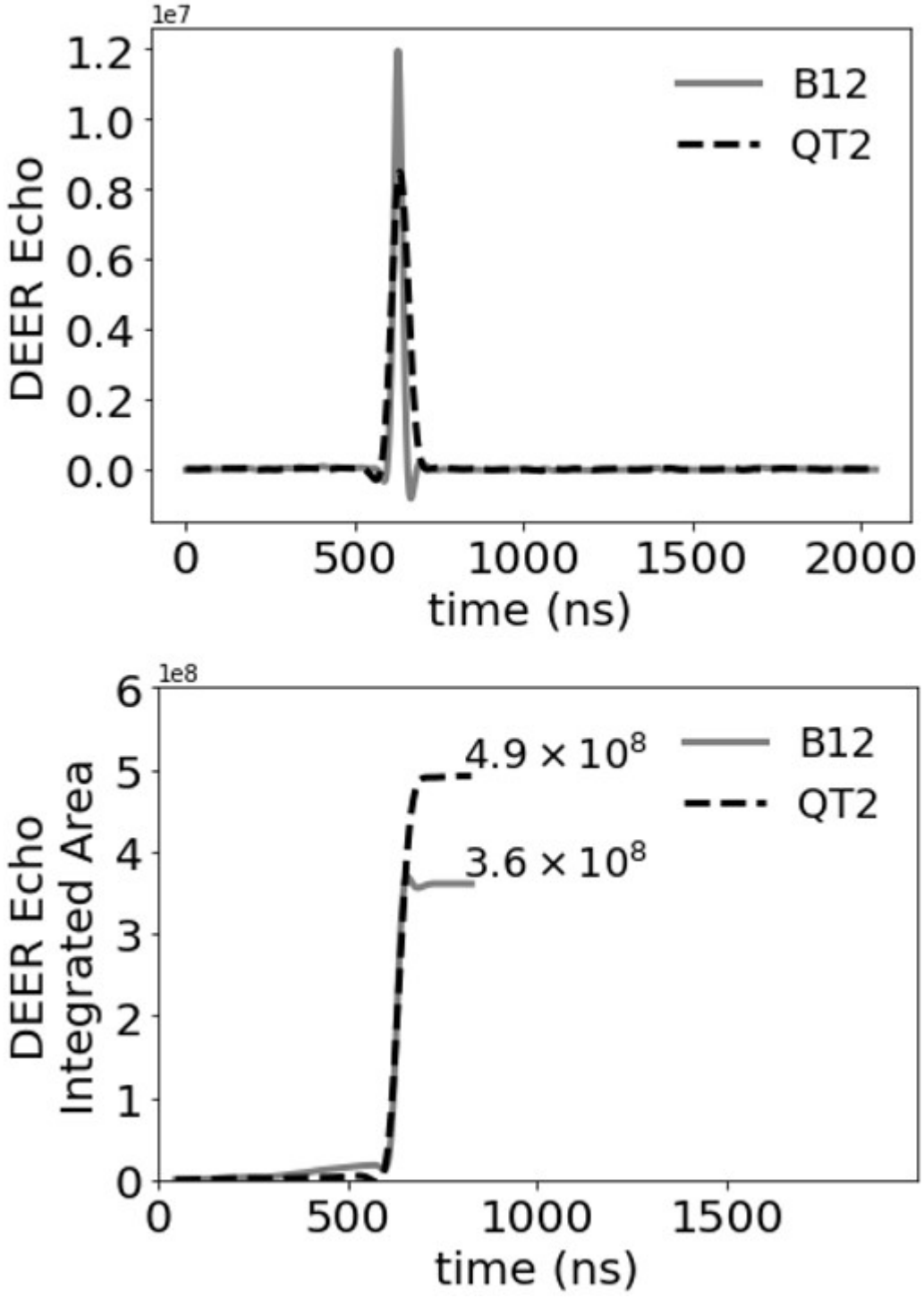

Figure S19. DEER echo was obtained using either QT2 (dashed black line) or B12 (solid gray line) resonator. The top panel shows the DEER echoes, while the bottom panel shows the integrated area of the echoes. Overall, despite B12 using 5 times fewer absolute spins than QT2, the echo area from B12 is about ~1/4 less than the echo obtained from QT2.

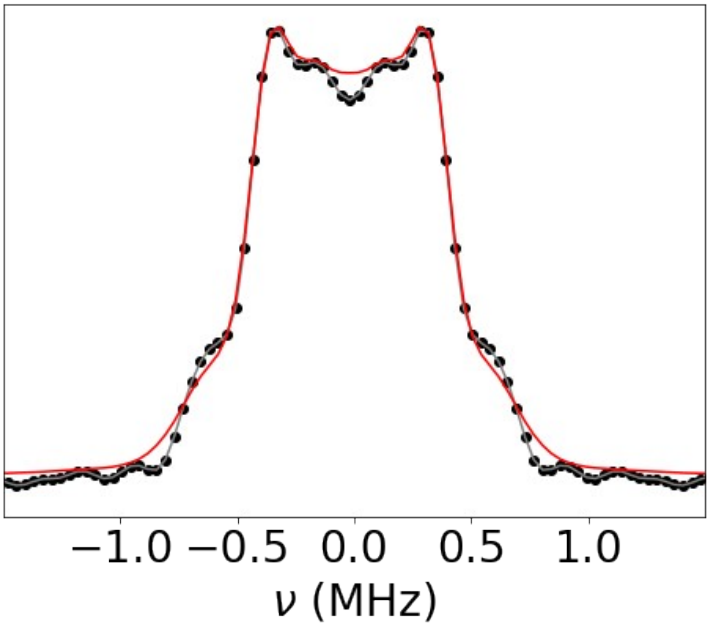

Figure S20. The spectrum of the summed DEER of dHis-Cu(II)-labeled hGSTA1-1. The black dots and gray line represent the experimental spectrum while the red line represents the fit from DeerAnalysis[2].

Bibliography

1. Breitgoff, F. D. *et al.* UWB DEER and RIDME distance measurements in Cu(II)-Cu(II) spin pairs. *J. Magn. Reson.* **308,** 106560 (2019).

2. Jeschke, G. *et al.* DeerAnalysis2006—a comprehensive software package for analyzing pulsed ELDOR data. *Appl Magn Reson* **30,** 473–498 (2006).